IMPACT-INDUCED CLAY MINERAL FORMATION AND DISTRIBUTION ON MARS. E. G. Rivera-Valentin[1], P. I. Craig[2]; [1]Arecibo Observatory, Universities Space Research Association, Arecibo, PR, 00612; [2]NASA Johnson Space Center, 2101 E. NASA Parkway, Houston, TX 77058. *ed@naic.edu*

Introduction: Clay minerals have been identified in the central peaks and ejecta blankets of impact craters on Mars [e.g. 1,2]. Several studies have suggested these clay minerals formed as a result of impact-induced hydrothermalism either during Mars' Noachian era or more recently by the melting of subsurface ice [3-6]. Examples of post-impact clay formation is found in several locations on Earth such as the Mjølnir [7] and Woodleigh Impact Structures [8]. Additionally, a recent study has suggested the clay minerals observed on Ceres are the result of impact-induced hydrothermal processes [9]. Such processes may have occurred on Mars, possibly during the Noachian.

Distinguishing between clay minerals formed pre- or post-impact can be accomplished by studying their IR spectra [10,11]. In fact, [10] showed that the IR spectra of clay minerals is greatly affected at longer wavelengths (i.e. mid-IR, 5-25 μm) by impact-induced shock deformation while the near-IR spectra (1.0-2.5 μm) remains relatively unchanged. This explains the discrepancy between NIR and MIR observations of clay minerals in martian impact craters noted in [12]. Thus, it allows us to determine whether a clay mineral formed from impact-induced hydrothermalism or were pre-existing and were altered by the impact [10]. Here we study the role of impacts on the formation and distribution of clay minerals on Mars via a fully 3-D Monte Carlo cratering model [13,14], including impact-melt production using results from modern hydrocode simulations [15]. We identify regions that are conducive to clay formation and the location of clay minerals post-bombardment.

Impact Model: Mars is modeled as a Cartesian sphere of radius 3390 km discretized into cubic volume elements 10 km on a side. We use Monte Carlo methods to select a population of impactors with a size-frequency distribution similar to the present-day asteroid belt and model the bombardment following the E-belt hypothesis [16,17]. The total bombardment mass incident on Mars is constrained using the estimated lunar bombardment mass, $\sim 3.5 \times 10^{19}$ kg [17], assuming Mars receives $\sim 2.76\times$ more material than the Moon [18]. Though it receives more impactors due to its proximity to the asteroid belt, the mean impact velocities on Mars is $\sim 0.54\times$ that of the Moon [18]. Impact velocity is thus modeled following a Rayleigh distribution about a mean value of 7 km/s and 11 km/s for the pre- and post-LHB eras, respectively.

Once chosen per run, the synthetic impactor populations are converted to crater populations following a Pi scaling law [19], where a projectile of diameter D and density ρ_i impacting at velocity v_i produces a crater of transient diameter

$$D_{tc} = 1.16 \left(\frac{\rho_i}{\rho_m} \right)^{\frac{1}{3}} D^{0.78} \left(v_i \sin\Omega \right)^{0.43} g^{-0.22}, \quad (1)$$

where $(\rho_i/\rho_m) \approx 1$, $g = 3.7$ m s^{-2} is Mars' gravity, and Ω is impact angle, which is randomly selected following a distribution of $d\Omega = \sin 2\Omega$. Impact location for every projectile onto the simulated Mars is chosen randomly for longitude and for latitude follows $d\phi = \sin 2\phi$. An impactor excavates and ejects material within a volume approximated as an oblate spheroid of depth $D_{tc}/8$, which is emplaced within an ejecta blanket modeled as an annulus surrounding the transient crater extending D_{tc} from the impact point. Impact melt is modeled following the scaling relationships from [15] such that an impactor of radius r_p produces a volume of melt at a depth of

$$z = r_p a_\zeta \left(\frac{v_i}{40\text{km/s}} \right)^{b_\zeta}, \quad (2)$$

where $a\zeta = 2.52$ and $b\zeta = 0.651$, of radius

$$r = r_p a_\chi \left(\frac{v_i}{40\text{km/s}} \right)^{b_\chi}, \quad (3)$$

where $a_\chi = 3.00$ and $b_\chi = 0.674$. Within the impact melt, clay mineral formation can occur and over time be redistributed across the surface.

Preliminary Model Results: For impactor populations with SFD characteristics like the asteroids belt, the bulk of the impacting mass is characterized by $D \approx 100$ km, of which there are ~ 70 such impacts on Mars. Following Equations 2-3, the bulk of the impact melt volume would then be characterized by $z \sim 50$ km and $r \sim 55$ km such that a total of $\sim 5 \times 10^7$ km^3 impact melt volume is produced during Mars' bombardment history. This is equivalent to ~ 0.2 km think global layer of melt. In Figure 1, we show an example simulation demonstrating the post-bombardment distribution of impact-melt on Mars, where P_{melt} is the volumetric probability of finding impact-melt. By our assumptions, this is the most likely area to find impact-formed clays. Though large impacts produce the most melt, their large excavation volume implies efficient mixing with undisturbed material. Smaller impacts, though, can more easily eject these melt volumes [20].
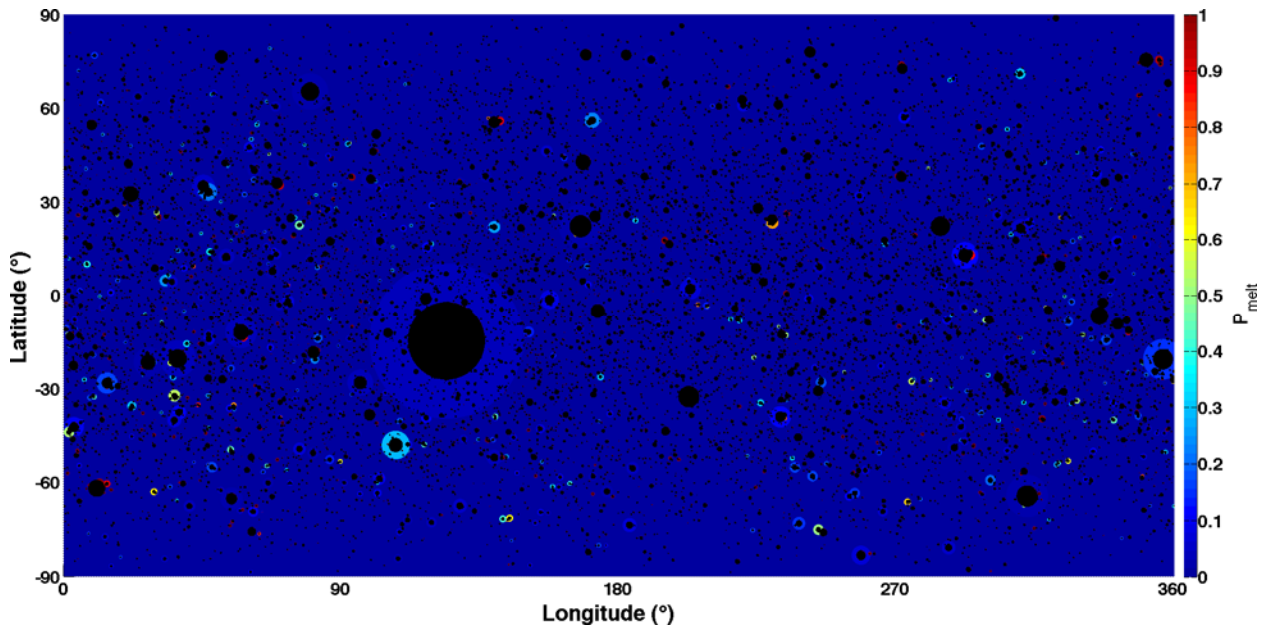
Figure 1: Post-bombardment distribution of impact-melt on Mars from a single impact history. The colors represent Pmelt. Crater floors, where mass-wasting, which is not included in the model, likely modifies the composition, are denoted by black.

For this simulation, on average P_{melt}=0.03. Thus, though Mars receives a lot more impacting mass than the Moon, the small impact velocity combined with the large surface area result in a small probability of finding impact melt relative to the Moon.

Implications for Mars: Clay minerals have been identified by their NIR spectral signature in the central peaks and rims of impact craters on Mars [e.g. 1,2,21]; however, this spectral signature results from only the first few μm depth of the surface and the absolute volume of the clay mineral is not certain. In our model, where there is impact melt, there is a possibility of forming clay minerals, but not all of that model volume will result in clay mineral formation. Our modeled P_{melt} is thus an upper bound probability of finding clay minerals.

Though most melt is made by large impacts, a large amount of undisturbed material is also excavated, so the ejecta is a mixture of both. Smaller, later impacts near these large basins excavate the basin melt and because their excavation volume is small is dominated by it resulting in high P_{melt} (red areas in Fig. 1). The resulting higher P_{melt} around smaller, younger impacts suggests areas of higher probability of clay mineral formation. In fact, a comprehensive study by [22] showed that given its slightly alkaline conditions (pH 6-8), hydrothermal systems resulting from terrestrial impacts are more likely to form clay minerals in smaller craters (D ≤ ~65 km).

Future Work: The model result presented here are only one possible scenario in which clay minerals can result from post-impact hydrothermal activity. We expect that different starting conditions (e.g. target rock composition, water content) in the model will yield different results. From this further work, we expect to be able to constrain the conditions under which clay minerals can form from impact-induced hydrothermal systems and the (re-)distribution of such clay minerals in the impact ejecta.

References: [1] Mangold N. et al. (2007) *JGR 112*, E08S04. [2] Loizeau D. et al. (2012) *Icarus 219*, 476-497. [3] Marzo G. et al. (2010) *Icarus 208*, 667-683. [4] Gross C. et al. (2012) *LPSC XLIII*, #1795. [5] Ehlmann B. et al. (2011) *Nature 479*, 53-60. [6] Fairen A. et al. (2010) *PNAS 107*, 12095-12100. [7] Dypvik H. and Ferrell R. (1998) *Clay Min. 33*, 51-64. [8] Uysal I. et al. (2000) *EPSL 192*, 281-289. [9] Zolotov M. (2014) *Icarus 228*, 13-26. [10] Gavin P. et al. (2013) *JGR 118*, 65-80. [11] Friedlander L. et al. *JGR, under review*. [12] Michalski J. et al. (2010) *Icarus 206*, 269-289. [13] Rivera-Valentin and Barr (2014) *EPSL 391*, 234-242. [14] Rivera-Valentin E. G. and Barr A. C. (2014) *ApJL* 782:L8. [15] Barr A. C. and Citron R. (2011) *Icarus* 211, 913-916. [16] Bottke W. F. et al. (2012) *Nature* 485, 78-81. [17] Morbidelli A. et al. (2012) *EPSL* 355-356, 144-151. [18] Le Feuvre M. and Wieczorek M. A. (2011) *Icarus* 214, 1-20. [19] Ivanov B. A. et al. (2002) *in Asteroids III*, 89-101. [20] Barnhart C. J. and Nimmo F. (2011) *JGR* 116, E01009. [21] Noe Dobrea E. et al. (2012) *GRL 39*, L23201. [22] Naumov M.V. (2005) *Geofluids 5*, 165-184.